BUTTERWORTH HEINEMANN

Polymer Vol. 36 No. 17, pp. 3359–3368, 1995

0032-3861/95/$10.00 + 0.00

Toughened polymer blends composed of a ductile styrene–butadiene–styrene matrix with brittle methyl methacrylate–styrene particles

Ikuro Yamaoka
Advanced Materials and Technology Research Laboratories, Nippon Steel Corporation, 1618 Ida, Nakahara-ku, Kawasaki 211, Japan
(Received 26 October 1994; revised 15 February 1995)

Screw-extruded polymer blends of poly(styrene-*block*-butadiene-*block*-styrene) triblock copolymer (KR05) with methyl methacrylate–styrene copolymer (MS-200) were injection moulded, and the mechanical properties and morphology were examined. KR05 is toughened by incorporation of MS-200, and synergistic improvement of toughness is observed for blends of KR05 matrix with MS-200 inclusions. Under tensile stress the KR05 matrix of the injection-moulded blends shows the same structural change as injection-moulded KR05 (extensive shear yielding). However, the blends also show cavitational breakdown in the polybutadiene phase and numerous outbreaks of minute debonding in the interfacial region between the KR05 matrix and MS-200 particles. These microscopic tearing phenomena could restrain excessive stress concentration and dissipate large energy before macrocrack propagation, leading to synergistic toughening.

(Keywords: styrene–butadiene–styrene; methyl methacrylate–styrene; impact strength)

INTRODUCTION

In heterogeneous polymer blends, mechanical properties, especially impact resistance, are related to morphological structure, in which microphase separation and a finely dispersed phase are present. The toughness of brittle polymers can be effectively improved by appropriate incorporation of a rubbery component in the form of particles[1], or else a network or a honeycomb structure[2]. In rubber-toughened blends with a brittle matrix such as polystyrene (PS), poly(methyl methacrylate) (PMMA) and styrene–acrylonitrile copolymer (SAN), dispersed rubber particles act as effective stress concentrators and mainly enhance crazing in the matrix on impact if both the rubber particle size and the rubber–matrix adhesion are adequately controlled[3]. In the other type of rubber-toughened blends with a ductile matrix such as nylon, poly(ethylene terephthalate) (PET) and polycarbonate (PC), the rubber particles mainly enhance shear yielding in the matrix on impact, when the surface-to-surface interparticle distance is smaller than the critical value[4–6]. Since both processes of crazing and shear yielding dissipate large amounts of impact energy, superior resistance to crack propagation can be achieved[2,7–12].

Several basic criteria for effective toughening of polymers have been developed in earlier works. While interest has been mainly concentrated on rubber-toughened blends[4,13–19], a new type of toughened polymer blend has recently been studied; these blends are composed of a ductile matrix with brittle polymeric particles[20–24]. They are termed 'brittle-in-ductile' blends in this paper. The 'brittle-in-ductile' blends may be toughened in a different manner from rubber-toughened blends. Impact energy can be absorbed by large plastic deformation of the brittle particles dispersed in the matrix[20]. Such cold drawing of a brittle polymeric inclusion could occur based on the von Mises criterion for yielding, as a result of stress concentration developed by bulk deformation only when adequate differences in both Young's modulus and Poisson's ratio are obtained between the matrix and the particles[21,22]. Such a toughening mechanism was shown in blends of PC as the ductile matrix with inclusions of SAN, PMMA, acrylonitrile–butadiene–styrene copolymer (ABS) or PS, blends of poly(butylene terephthalate) (PBT) with inclusions of SAN or PMMA, and also a nylon-6 blend with inclusions of SAN[20,21,23,24].

It is of more interest to consider 'brittle-in-ductile' blends with a ductile matrix of a commodity polymer, because those are expected to be more easily processable and often cost-effective. Styrene-enriched styrene–butadiene block copolymer could be one of the candidates as the ductile matrix. This type of block copolymer is found to be toughened by incorporation of adequate brittle polymers, although few related studies seem to have been carried out[25]. In the present paper, the toughness–morphology relationship has been examined for 'brittle-in-ductile' blends composed of poly(styrene-*block*-butadiene-*block*-styrene) triblock copolymer (SBS) with methyl methacrylate–styrene random copolymer (MS) as a source of brittle inclusions.

EXPERIMENTAL

Materials

A commercial star-shaped poly(styrene-*block*-butadiene-*block*-styrene) triblock copolymer (SBS) manufactured by Phillips Petroleum Co. under the tradename of K-Resin KR05 was used here. A star-shaped block copolymer was chosen because it has the advantage of better stiffness than linear block copolymers of equivalent styrene/butadiene composition and block molecular weights[26]. The number- and weight-average molecular weights (M_n and M_w) and their ratio (M_w/M_n) for KR05, using g.p.c., are 5.23×10^4, 1.51×10^5 and 2.89, respectively. N.m.r. measurements revealed that KR05 has a 0.245 weight fraction of the polybutadiene (PB) block component. Measurements by d.s.c. showed two distinct glass transitions (T_g) near −80 and 95°C corresponding to the PB phase and the PS phase, respectively.

KR05 was melt mixed with a commercial methyl methacrylate–styrene copolymer (MS) supplied by Nippon Steel Chemical Corp. under the tradename of MS-200. The number- and weight-average molecular weights (M_n and M_w) and their ratio (M_w/M_n) for MS-200 are 1.00×10^5, 2.30×10^5 and 2.30, respectively, using g.p.c. The weight fraction of the styrene component is 0.78. The polymers were used as received.

Sample preparation

Extrusion. KR05 was melt mixed with different weight ratios of MS-200 dried in an oven at 80°C for 4 h. A partially intermeshing, counter-rotating twin-screw extruder ($D = 20$ mm, $25D$ screw without mixing sections; Toyo Seiki Seisaku-sho Ltd) was used for melt mixing at 220°C with a screw speed of 70 r.p.m. Extruded strands were quenched in a water trough and pelletized. Tension was applied to the melt strands for stable pelletization. As-received KR05 and MS-200 were also extruded to give the same thermal history as for the blends. In this paper, pellets extruded once are termed 'once-extruded' pellets.

Good dispersion on extrusion could not be attained as the extruder used was equipped with no effective mixing sections on full-flighted screws. Mixedness of 'once-extruded' KR05/MS-200 blends could be improved through re-extrusion, in which dried 'once-extruded' pellets were re-extruded in the same way as mentioned above. Re-extruded pellets are termed 'twice-extruded' pellets.

The compositions of the blends are indicated as weight percentages KR05/MS-200. For example, KR05/MS-200 (85/15) represents a blend of 85 wt% KR05 and 15 wt% MS-200.

Injection moulding. 'Once-' and 'twice-extruded' pellets were injection moulded (Toshiba Machinery IS100E injection moulding machine) into impact, tensile and flexural test bars with the corresponding thicknesses of 6.35 mm (0.25 inch), 3.2 mm (0.125 inch) and 6.35 mm (0.25 inch), respectively. Flexural test bars were used for the measurement of deflection temperature under flexural load, too. Barrel temperature, mould temperature and injection rate were set at 210°C, 40°C and 40 $cm^3 s^{-1}$, respectively.

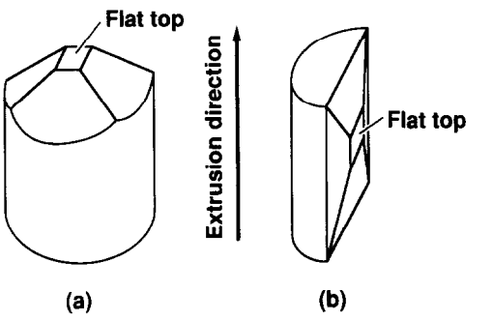

Figure 1 Diagram showing pyramid-shaped pieces cut from pellets. Flat tops on the pieces (a) and (b) were made for microtoming normal and parallel to the extrusion direction, respectively

Mechanical tests

The notched Izod impact strength was measured at 23°C according to ASTM D256 using a pendulum-type tester. Tensile and three-point loading flexural tests were carried out on a conventional Instron testing machine at 23°C according to ASTM D638 and ASTM D790, respectively. The deflection temperature under flexural load was measured under a maximum fibre stress of 1820 kPa according to ASTM D648.

Examination of morphology

Morphologies of the polymer extrudates and their mouldings were observed with transmission electron microscopy (TEM). Cylindrical 'once-' and 'twice-extruded' pellets were machined into pyramid-shaped pieces, as shown in *Figure 1*. Their apexes were cut off for later microtoming, in order to expose surfaces normal (*Figure 1a*) or parallel (*Figure 1b*) to the extrusion direction on flat tops of the pieces. *Figure 2* shows a pyramid-shaped piece cut out of an injection-moulded impact test bar. The Y axis was fixed parallel to the melt flow direction during injection moulding. Apexes of the pieces were cut off to expose the surfaces of the XY plane on the resultant flat tops. All the surfaces of interest were made near core regions of the pellets or bars. After treatment with a 2% aqueous solution of osmium tetroxide to stain the PB phase of KR05, ultra-thin sections (500–900 Å thick) were cut from the flat tops of the pieces using an LKB microtome with a diamond knife. Sections were observed with a Hitachi H700 transmission electron microscope at an accelerating voltage of 100 kV. Routine magnifications of 30 000× and 100 000× were adopted.

The morphology of injection-moulded tensile bars after stress application was examined in the same way as reported previously[27].

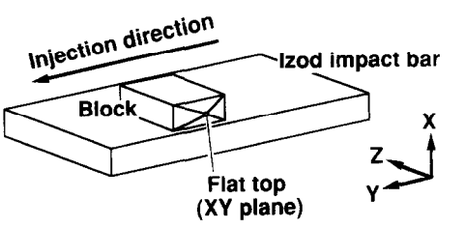

Figure 2 Diagram showing a pyramid-shaped piece cut from an injection-moulded plaque. A flat top on the piece was made for microtoming parallel to the injection direction

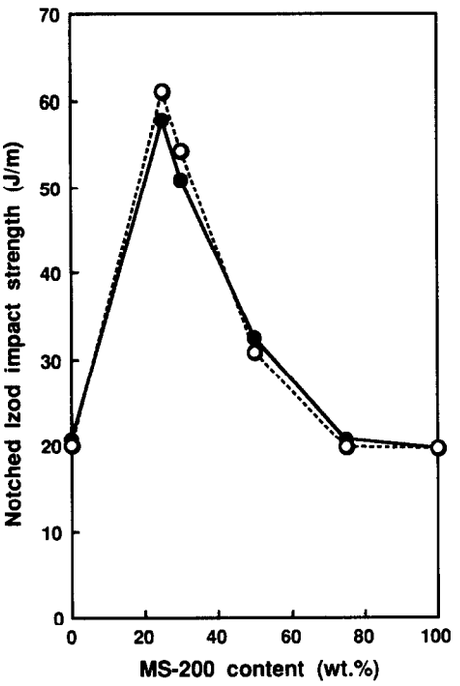

Figure 3 Notched Izod impact strength of KR05/MS-200 blends plotted as a function of MS-200 content. Filled and open circles represent the data for injection mouldings of 'once-' and 'twice-extruded' pellets, respectively

RESULTS AND DISCUSSION

Mechanical properties

Figure 3 shows the notched Izod impact strength of injection mouldings of 'once-' and 'twice-extruded' pellets of KR05/MS-200 blends. KR05 is toughened by incorporation of MS-200. The impact strength exhibits synergistic improvement and goes through a maximum between 10 and 40 wt% MS-200. Very little difference in impact strength is seen between injection mouldings of 'once-' and 'twice-extruded' pellets with the corresponding blending ratio. *Figure 4* shows the tensile strength and the flexural modulus of injection mouldings of 'once-extruded' pellets. The deflection temperature of those mouldings under flexural load is shown in *Figure 5*. No synergistic effects are seen for those rigidity-related properties of the blends as MS-200 is added to KR05. Structural features of KR05/MS-200 blends could account for those results, which is discussed later.

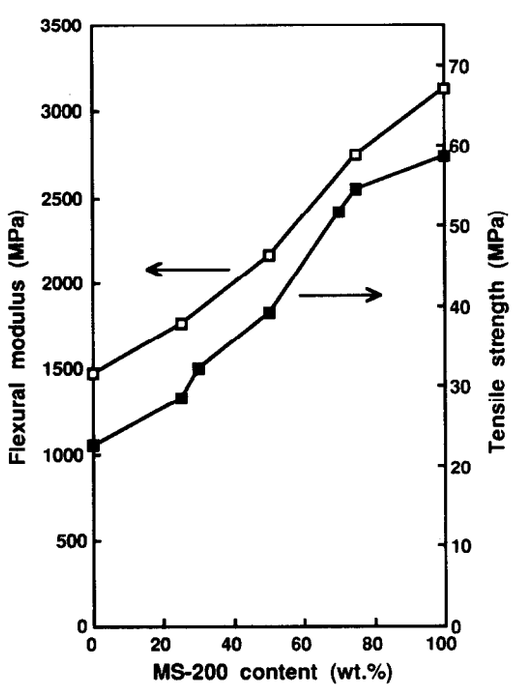

Figure 4 Tensile strength (filled squares) and flexural modulus (open squares) of KR05/MS-200 blends plotted as a function of MS-200 content

Morphology of extrudates

Figures 6 and *7* are transmission electron micrographs showing morphologies of 'once-' and 'twice-extruded' pellets of KR05/MS-200 (85/15) blends, respectively. In these figures (a-1) and (b-1) are micrographs taken on surfaces normal and parallel to the extrusion direction, respectively; (a-2) and (b-2) are higher-magnification views of (a-1) and (b-1), respectively. The extrusion directions are shown with arrows on (b-1) and (b-2). The island–matrix morphologies have three distinct phases: unstained MS-200 dispersed phase macrophase-separated from the KR05 matrix, and PS and PB phases microphase-separated in KR05. Note in this paper that the terms 'macro-' and 'microphase separation' indicate inter- and intrapolymer phase separation, respectively[28,29]. The KR05 phase in the blends exhibits the same lamellar-type phase separation as seen in injection-moulded KR05[27]. Both the stained PB phase and the bright PS phase form alternating lamellae of thicknesses 150–200 Å and 200–250 Å, respectively. Detailed observation of the morphology revealed that the microphase separation in KR05 is not complete since in KR05 many parts of PB lamellae are disconnected in the PS matrix phase. KR05 lamellae are disordered in the wavy form since KR05, which should be microphase-separated to form lamellae in the melt exiting the extruder die at the extrusion temperature adopted here (220°C)[27], was quenched and solidified rapidly in a disequilibrium

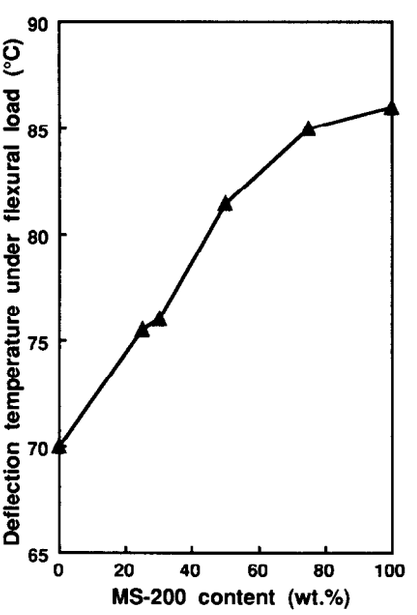

Figure 5 Deflection temperature of KR05/MS-200 blends under flexural load plotted as a function of MS-200 content

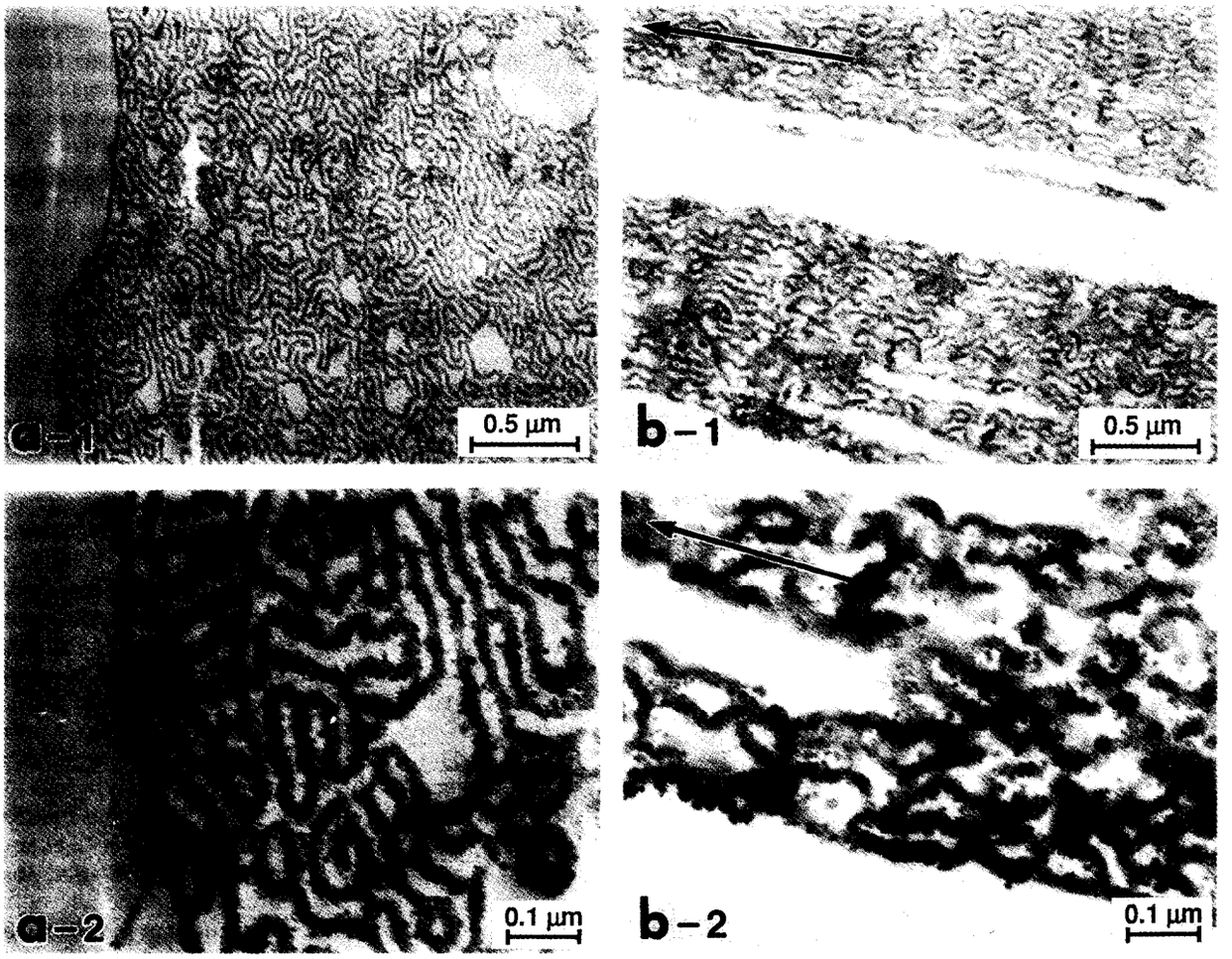

Figure 6 Transmission electron micrographs of 'once-extruded' pellets of KR05/MS-200(85/15) blends. Micrographs (a) and (b) show morphology observed on surfaces normal and parallel to the extrusion direction, respectively. The extrusion directions are shown with arrows on (b). Micrographs (a-2) and (b-2) are higher-magnification views of (a-1) and (b-1), respectively

state under intensive extensional stress and a large temperature gradient.

Macrophase separation of KR05/MS-200 blends is related to the interaction of MS-200 with block components of KR05. We refer to two factors that are influential in forming macrophase morphology of KR05/MS-200: compatibility between the two polymers, and potential solubility of MS-200 in the compatible block phase of KR05. In an equilibrium state these factors are not strongly correlated with each other, as discussed later. From the difference of compatibility with MS-200 between the PS and the PB blocks of KR05, we can judge which block is more favourable to MS-200. If we can ignore the effects of the chemical linkage between the two blocks on the compatibility of KR05 with MS-200, this matter can be argued on the grounds of the difference in compatibility with MS-200 between PS homopolymer and PB homopolymer. MS-200 could be rather compatible with PS homopolymer because of the large fraction of styrene (78 wt%) in MS-200[30] and the very weak repulsion between the MMA units of MS-200 and the styrene units of PS. The χ interaction parameter χ_{M-S} between MMA and styrene units is very small, of the order of 0.1–0.2[31–33]. The polymer–polymer interaction parameter χ_{blend} between PS and MS can be derived[34,35] as:

$$\chi_{blend}^{PS/MS} = x^2 \chi_{M-S}$$

where x is the MMA weight fraction in MS. Actually, $\chi_{blend}^{PS/MS-200} \approx (0.22)^2(0.2) \approx 0.01$ is comparable to χ_{blend} of other compatible blends such as PC/PMMA[36] (0.036–0.047) and PC/SAN[37] (0.031–0.037, SAN containing 23% acrylonitrile), and even comparable to that of miscible PPO/PS[38] (0.005). Thus, we can expect the MS-200 to be compatible with PS. Intuitively we can guess that MS-200 is repulsive to PB because of the slight molecular resemblance between the two. Accordingly, in KR05/MS-200 blends MS-200 could be much more attractive to the PS block than to the PB block of KR05. The KR05/MS-200 interface could be formed between the PS block phase of KR05 and the MS-200 phase.

Macrophase separation seen in polymer blends often resembles the poor compatibility between the component polymers of blends. However, when macrophase separation is observed in blends composed of block copolymer A–B and polymer C compatible with the A block of the A–B copolymer, such as KR05/MS-200, this could often be in large part due to limited solubilization of the C polymer into the A block phase rather than to the degree of compatibility between the C polymer and

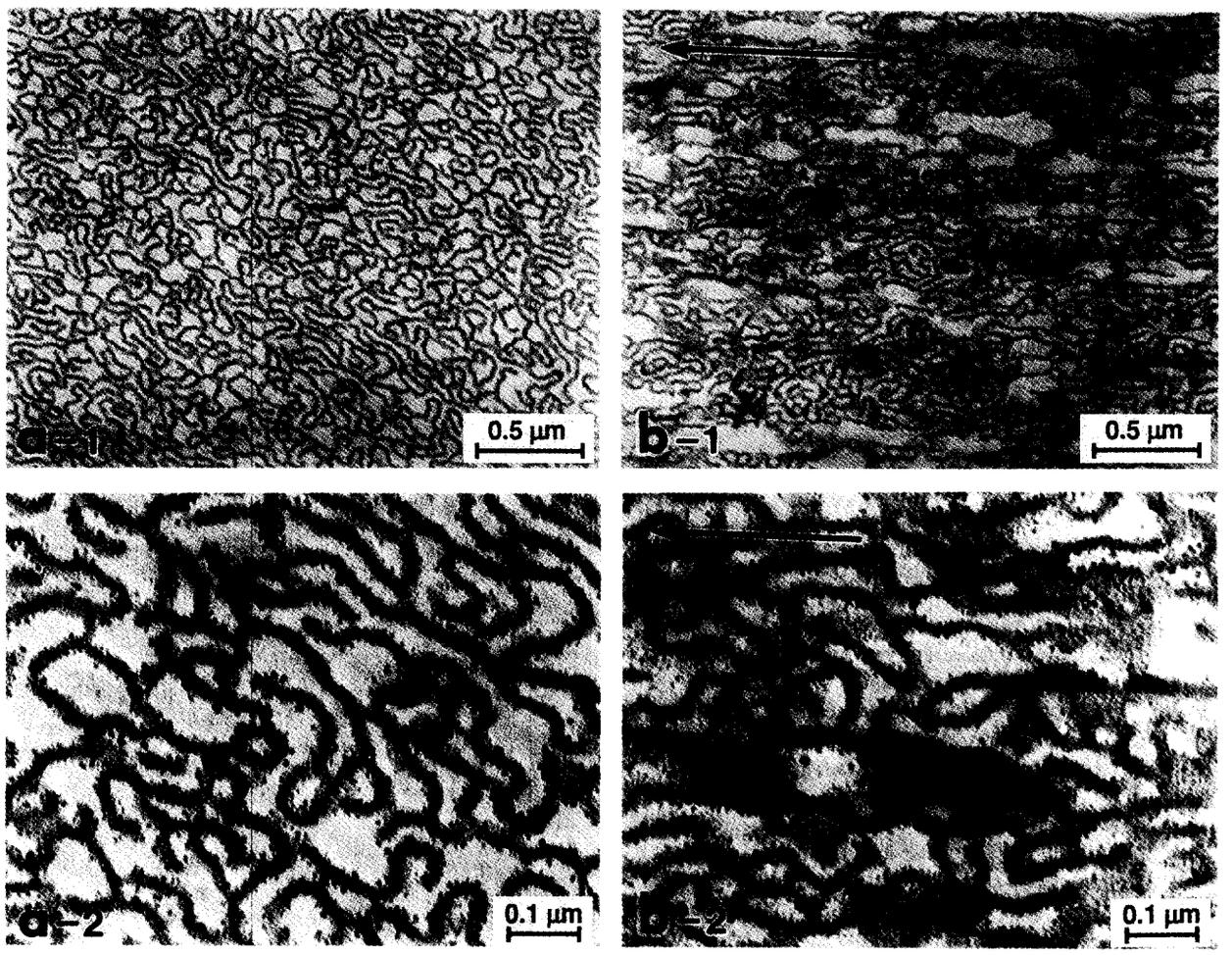

Figure 7 Transmission electron micrographs of 'twice-extruded' pellets of KR05/MS-200(85/15) blends. Micrographs (a) and (b) show morphology observed on surfaces normal and parallel to the extrusion direction, respectively. The extrusion directions are shown with arrows on (b). Micrographs (a-2) and (b-2) are higher-magnification views of (a-1) and (b-1), respectively

the A block. For such blends, degree of solubilization does not correspond to degree of compatibility. Even when the C polymer is much more compatible with the A block ($\chi_{blend}^{A/C} \approx 0$) or in a special case chemically equivalent to the A block ($\chi_{blend}^{A/C} = 0$), limited solubilization may often cause macrophase separation. For the case in which the C polymer is the same as the A homopolymer, namely for A–B block copolymer/A homopolymer blends such as KR05/PS, Inoue *et al.*[39,40] derived an equation for the solubilizing free energy. They concluded that equilibrium in solubilization depends on (a) the solubilized volume fraction of A homopolymer, (b) the ratio of molecular weights of A homopolymer to the A block of A–B copolymer, and (c) the extension coefficient of the perturbed polymer chain of the A block, which represents relatively the excluded volume of the polymer chain of the A block. The effects of (b) have been examined by a number of researchers with TEM, small-angle X-ray scattering (SAXS) and/or small-angle neutron scattering (SANS)[39,41–44]. By using these devices, macrophase separation was observed in A–B block copolymer/A homopolymer blends when, as a rule of thumb, the molecular weight of the A homopolymer exceeds that of the A block of the copolymer[39,41,44]. It should be noticed that, even when the molecular weight of the A homopolymer is much larger than that of the A block of the A–B copolymer, a small degree of solubilization definitely occurs; however, the consequent change in domain size is too small to be discernible with TEM or SAXS[39].

We can judge whether MS-200 is solubilized well into the PS block phase of KR05 by considering solubilization phenomena for KR05/PS blends. Since MS-200 is obviously less favourable to the PS block of KR05 than PS homopolymer is to the same PS block when the MS-200 and the PS homopolymer have the same molecular weight, the MS-200 is hard to solubilize into the PS block phase of KR05 as long as the PS homopolymer is not solubilized well into the same PS block phase. In other words the KR05/MS-200 blends are definitely macrophase-separated as long as the KR05/PS blends with the corresponding blending ratio are macrophase-separated. Gebizlioglu *et al.*[45] examined solubilization of PS into the PS block phase of K-Resin. They used KR01, which is also a star-shaped SBS in the K-Resin family but another grade than the KR05 used here. KR01 and KR05 have similar weight fractions of the PB block component, 0.23 and 0.245, respectively. Successful solubilization requires that the molecular

weight of the added PS homopolymer should be less than the average molecular weight of PS blocks in branch arms of the KR01 molecule[45]. For the KR05 with M_w of 1.51×10^5 used here, the average M_w of the arms is less than 5.03×10^4 ($= 1.51 \times 10^5/3$) since the star-shaped KR05 molecule has at least three arms. For a 0.755 weight fraction of the PS block component, the average M_w of the PS blocks in the KR05 arms is estimated at less than 3.80×10^4 ($= 5.03 \times 10^4 \times 0.755$, $M_{w,crit.}$). Consequently, the KR05/PS blends could be macrophase-separated when at a rough estimate the added PS homopolymer has M_w over 3.80×10^4. If the added PS is replaced by MS-200 with M_w over 3.80×10^4, the resultant KR05/MS-200 blends also could be macrophase-separated. The M_w of the MS-200 used (2.30×10^5) is definitely large enough to induce macrophase separation.

A hot melt of KR05/MS-200 blends at 220°C looked opaque when exiting the extruder die, but turned transparent gradually upon cooling down. This suggests that optically heterogeneous structure of the order of a few thousand ångströms or more in size should exist in the hot melt at the die exit[46], which scattered some visible light with wavelength between ca. 3800 Å and ca. 7600 Å. This is not attributed to microphase separation in the KR05 phase of the blends because the thickness of the KR05 lamellae that could exist at a mixing temperature of 220°C[27] is much smaller than the size interfering in the wavelength of visible light. In the die, a hot melt of KR05/MS-200 blends could be macrophase-separated between the molten KR05 phase and the molten MS-200 phase. Many parts of the two molten phases would be more than a few thousand ångströms in size. The two phases would differ considerably in refractive index at the mixing temperature, whereas they exhibit much the same refractive index at room temperature (1.572 and 1.570 for KR05 and MS-200, respectively), which results from the different temperature dependences of the refractive index between the two[47].

Only 'once extrusion' through the extruder resulted in a low degree of mixedness. MS-200 particles have a wide variety of sizes and show poor dispersion (*Figure 6*). A previous study emphasized that full-flighted screw extruders with no mixing sections bring about poor mixedness compared with those equipped with mixing sections[48,49]. This is responsible for coarser dispersions of MS-200 domains in 'once-extruded' pellets. After one more extrusion, however, fairly good mixedness of MS-200 particles with narrower size distribution was achieved (*Figure 7*).

Figure 8 shows the morphology of 'twice-extruded' pellets of KR05/MS-200 (75/25) and (50/50) observed on sections parallel to the extrusion directions, which are shown with the arrows. Addition of MS-200 tends to induce transitions from a morphology with MS-200 dispersed phase (KR05/MS-200 (85/15) and (75/25); see *Figures 7b* and *8a*, respectively) to that with co-continuous phases (KR05/MS-200 (50/50); *Figure 8b*). Phase inversion between KR05 and MS-200 would occur near a blending ratio of 50 wt% MS-200.

On all the micrographs of the pellets taken, the KR05/MS-200 interface was very wavy, and both the KR05 and the MS-200 phases were highly elongated in the extrusion direction (*Figures 6–8*). The microdomain structure with micro- and macrophase separation was

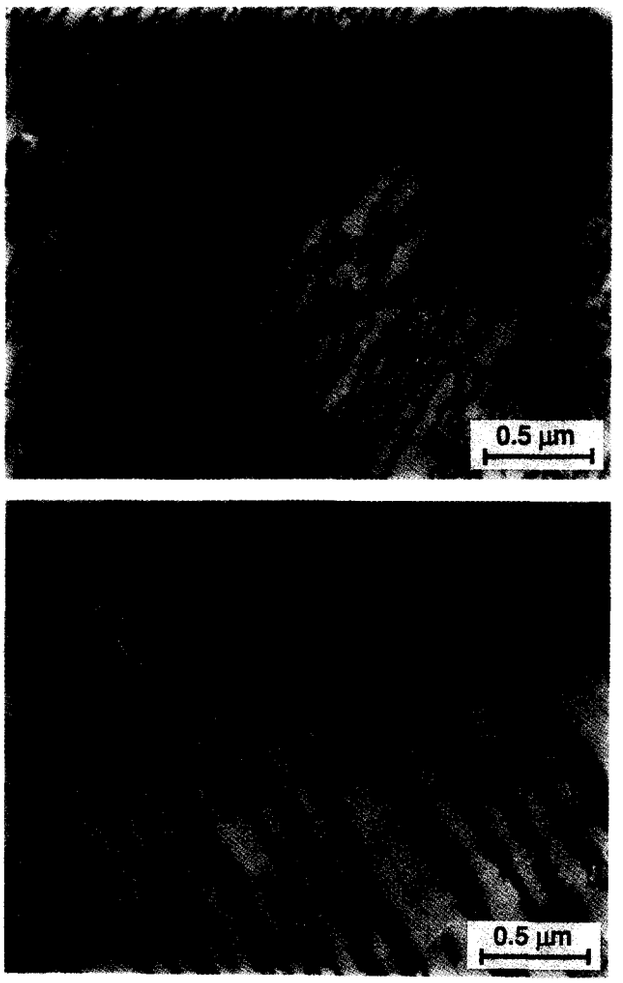

Figure 8 Transmission electron micrographs of 'twice-extruded' pellets of KR05/MS-200(75/25) and (50/50) blends: (a) (75/25); (b) (50/50). The morphology was observed on surfaces parallel to the extrusion directions, which are shown with arrows

settled in disequilibrium with the rapid variation of flow and temperature when the molten blends went through a strand die of the extruder and then were quenched, as mentioned above.

Morphology of injection mouldings

Morphologies of injection mouldings of 'once-' and 'twice-extruded' pellets are shown in *Figures 9* and *10*, respectively, for blends of KR05/MS-200 (70/30), (50/50) and (25/75) with that of neat KR05. They were observed on sections parallel to the injection direction (*Figure 2*), and found to be similar, except for the degree of elongation of domains, to those of 'twice-extruded' pellets observed on sections parallel to the extrusion direction (*Figures 7b* and *8*). The lamellae both of the KR05 phase in the blends and of neat KR05 are wavy and oriented in the injection directions (shown with the arrows on the micrographs) to a greater or lesser extent despite the morphology observed on sections from the core region of the injection mouldings. On injection moulding, the memory of the micro- and macrophase separations in the blends would not be initialized since the blends could be both micro- and macrophase-separated in the melt at the resin temperature of 210°C as

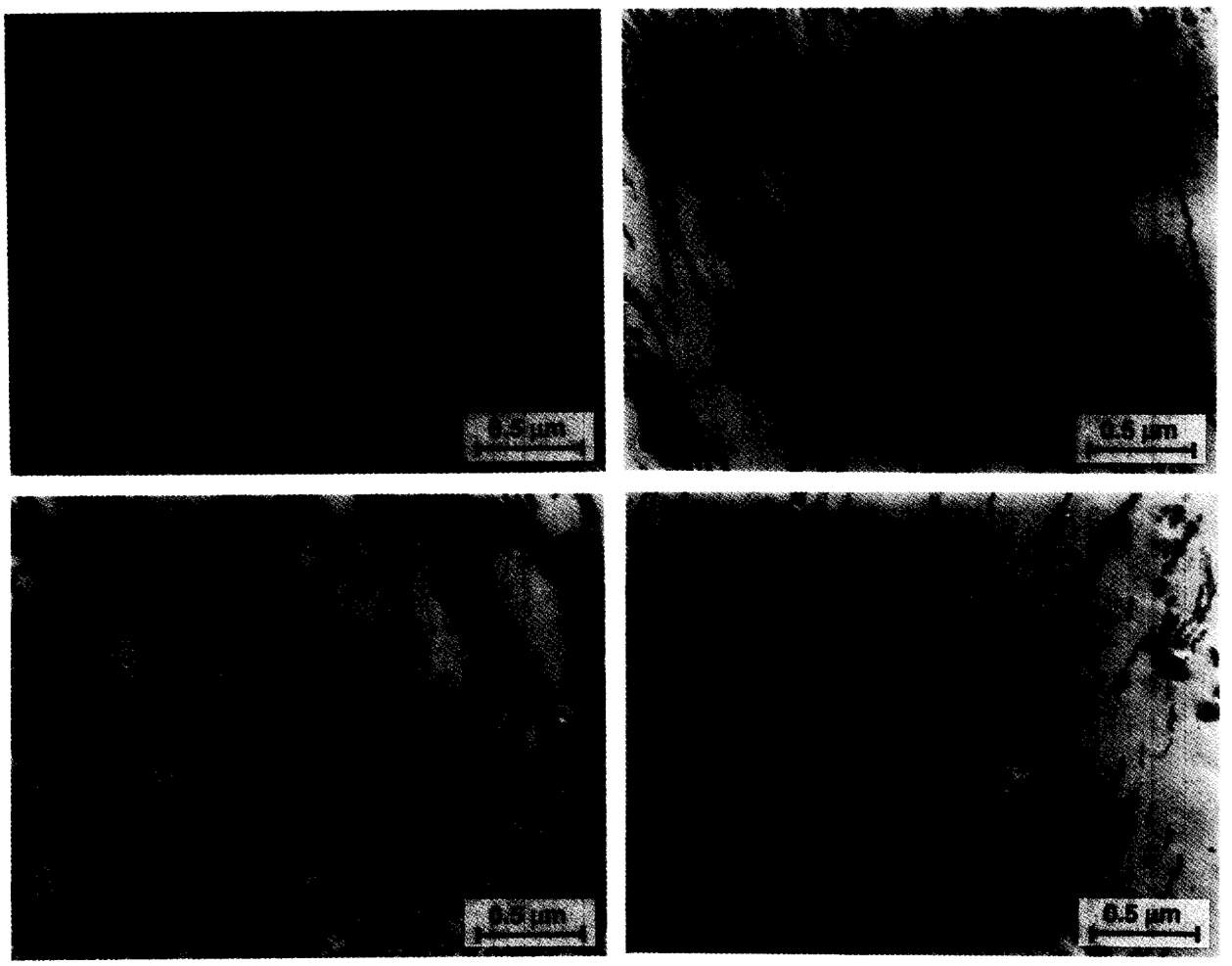

Figure 9 Transmission electron micrographs of injection mouldings of 'once-extruded' KR05/MS-200 blends: (a) (100/0); (b) (70/30); (c) (50/50); (d) (25/75). The morphology was observed on surfaces parallel to the injection directions, which are shown with arrows on respective micrographs

discussed above, and only reorientation of the KR05 lamellae and the MS-200 phases could occur. Such reorientation, which would be induced by shear flow behind the melt front on mould filling[50], could not be well relaxed on subsequent cooling because the melt viscosity increased very rapidly as the resin temperature fell in the cold mould.

As shown in *Figures 9* and *10*, addition of MS-200 to KR05 induces morphological transitions, from that with dispersed MS-200 particles (KR05/MS-200 (70/30)) to that with co-continuous phases ((50/50)) and, after phase inversion is completed, to that with the MS-200 matrix ((25/75)). No noticeable difference in morphology is seen between injection mouldings of 'once-' and 'twice-extruded' pellets with the corresponding blending ratio. High shear applied to the melt on injection moulding could enhance the degree of mixedness of 'once-extruded' pellets.

In *Figure 11* one can see the morphological change that resulted from tensile stress application to the injection-moulded specimen of KR05/MS-200 (70/30) blend. In *Figure 11* (a-1) and (a-2) show the morphology of an unstretched specimen of the mouldings; (a-2) is a higher-magnification view of (a-1). Arrows on the micrographs show the injection directions. Micrographs (b-1), (b-2), (b-3) and (b-4) show the deformation structure observed in the region just below the fracture surface after tensile stress application in the direction of the arrows at 50 mm min^{-1} up to the point of break. Stretching was done in the injection direction of the specimen. Micrographs (b-2), (b-3) and (b-4) are higher-magnification views of (b-1), and were taken at sites with ((b-2) and (b-3)) and without black dots ((b-4)). Micrograph (b-4) is added to see the deformation of KR05 lamellae clearly. Respective viewpoints taken for (b-2), (b-3) and (b-4) were a little way (only a few micrometres) from each other on the same cross-section. Comparison between the morphologies of an unstretched (*Figure 11a*) and a stretched (*Figure 11b*) specimen revealed considerable structural change on stretching. KR05 lamellae in an unstretched specimen of the blend (*Figure 11a*) are deformed irregularly by predominant shear yielding to destructive lamellae in a stretched one (*Figure 11b*). As mentioned for the deformation mechanism of KR05 injection mouldings in our previous study[27], the PS lamellae surrounding the intermittent PB lamellae in an unstretched state (*Figure 11a*) could be fragmented as the strain increased, and the consequent gradual phase inversion could result in separate PS domains dispersed in PB lamellae. In (b-2), (b-3) and (b-4) of *Figure 11*, larger arrowheads 1 and 2 point to some PS

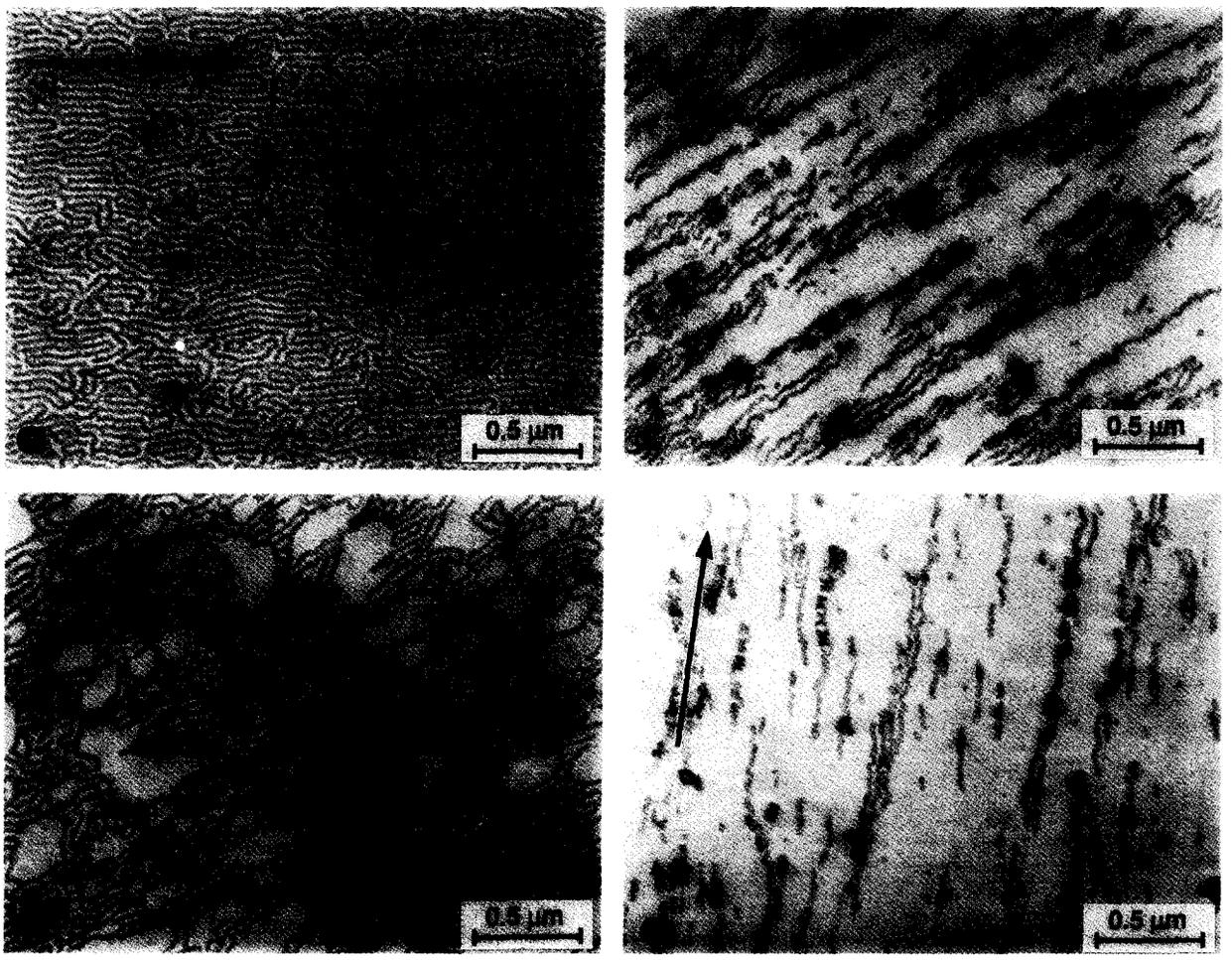

Figure 10 Transmission electron micrographs of injection mouldings of 'twice-extruded' KR05/MS-200 blends: (a) (100/0); (b) (70/30); (c) (50/50); (d) (25/75). The morphology was observed on surfaces parallel to the injection directions, which are shown with arrows on respective micrographs

domains and MS-200 particles surrounded by PB lamellae, respectively.

The black dots seen in the micrographs (*Figure 11b*) suggest that an early stage of cavitational breakdown in the PB phase, and in addition numerous outbreaks of minute debonding in the interfacial region between the KR05 matrix and dispersed MS-200 particles, resulted in preferential fixing by subsequent osmium tetroxide treatment[51]. In (b-2) and (b-3) of *Figure 11*, smaller arrowheads 3 and 4 point to some microcavities in the PB phase and the KR05/MS-200 interface region, respectively. These microcavities account for whitening (opacity) in the region near the fracture surface. After sufficient yielding development, final fracture could occur through the growth of microcavities into local microcracks and further macrocrack propagation. Since all the broken specimens examined showed the same structural changes as in *Figure 11*, macroscopic deformation of injection mouldings of KR05-enriched blends could occur through shear yielding of the KR05 matrix, cavitation in the PB phase and debonding in the KR05/MS-200 interfacial region. The growth of the cavitation and the debonding in the blends could restrain excessive stress concentration and dissipate large energy before macrocrack propagation. This should lead to synergistic toughening of KR05-enriched blends since no such microscopic tearing phenomena can be seen in the injection-moulded specimen of neat KR05[27]. Debonding in the interfacial region could be a more influential factor in synergistic toughening since the presumed good compatibility of the PS block of KR05 with MS-200, which could be considered regardless of limited solubilization of MS-200 into the PS block as mentioned above, could produce a strong interface between KR05 and MS-200.

Notched Izod impact data of injection mouldings of 'once-' and 'twice-extruded' pellets are much the same for the corresponding blending ratio (*Figure 3*). This could be due to morphological analogy between the corresponding mouldings in the two groups (*Figures 9* and *10*).

The tensile strength, flexural modulus and deflection temperature under flexural load of injection mouldings of KR05/MS-200 blends change linearly with the blending ratio (*Figures 4* and *5*). The coexistence of large positive deviation of impact strength (*Figure 3*) and no negative deviation of these rigidity-related properties from linear additivity should be emphasized. This phenomenon is not consistent with the conventional phenomena found for many polymer blends, in which enhanced toughness (namely, positive deviation of toughness) must be followed by degraded rigidity

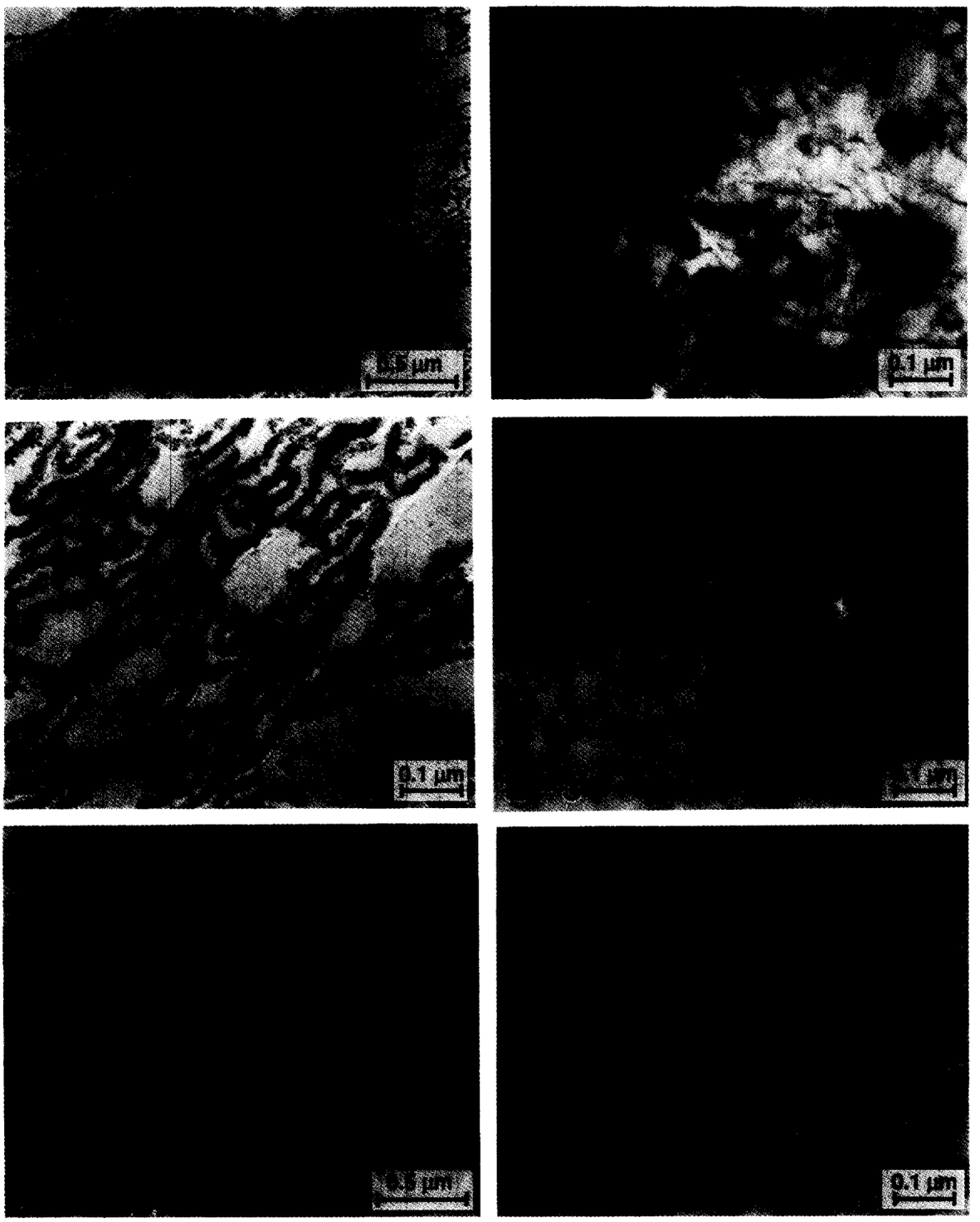

Figure 11 Transmission electron micrographs of an injection-moulded specimen of 'twice-extruded' KR05/MS-200(70/30) blend before tensile stress application ((a-1) and (a-2)) and after fracture under tensile stress ((b-1), (b-2), (b-3) and (b-4)). Morphological changes were observed on longitudinal cross-sections just below the fracture surface. Tensile directions are shown with double arrows on (b-1), (b-2), (b-3) and (b-4). Micrograph (a-2) is a higher-magnification view of (a-1); (b-2), (b-3) and (b-4) are higher-magnification views of (b-1), and were taken at sites with ((b-2) and (b-3)) and without black dots ((b-4))

(namely, negative deviation of rigidity). One reason for this would be large resistance to plastic deformation of the PB lamellae, which must be due to the close and complicated networks of rigid PS lamellae tangled with PB lamellae in the KR05 phase. Mouldings of neat KR05 with such complicated lamellar networks are obviously more rigid than those with orderly lamellae[27]. Another reason would be effective adhesion lasting at the KR05/MS-200 interface under deformation before cavitational regions spread predominantly.

CONCLUSIONS

Injection mouldings of KR05/MS-200 blends show synergistic improvement of toughness for KR05-enriched composition. The morphological structure of the blends consists of three distinctive phases: the MS-200 phase macrophase-separated from the KR05 phase, and the PS and PB phases microphase-separated from each other in KR05. The three phases are highly elongated in both extrudates and injection mouldings, since those phases existing even in the melt are subjected to the shear or extensional flow field occurring on melt processing and subsequent cooling. When tensile stress is applied to injection mouldings of KR05-enriched blends, KR05 lamellae shear yield extensively. The blends also show microcavitation in the PB phase and minute debonding in the KR05/MS-200 interfacial region. These microscopic tearing phenomena could avoid excessive stress concentration and dissipate large energy before fracture, responsible for synergistic toughening.

REFERENCES

1 Bucknall, C. B., 'Toughened Plastics', Applied Science, London, 1977
2 Menges, G. *Makromol. Chem., Macromol. Symp.* 1989, **23**, 13
3 Fowler, M. E., Keskkula, H. and Paul, D. R. *Polymer* 1987, **28**, 1703
4 Wu, S. *Polymer* 1985, **26**, 1855
5 Margolina, A. and Wu, S. *Polymer* 1988, **29**, 2170
6 Wu, S. *Polym. Eng. Sci.* 1990, **30** (13), 753
7 Bucknall, C. B., Clayton, D. and Keast, W.E. *J. Mater. Sci.* 1972, **7**, 1443
8 Yee, A. F. Int. Symp. on Toughness, Fracture and Fatigue of Polymers and Composites, Yamagata Univ., Japan, 1990, Abstract, p. 4
9 Bucknall, C. B. Int. Symp. on Toughness, Fracture and Fatigue of Polymers and Composites, Yamagata Univ., Japan, 1990, Abstract, p. 30
10 Takemori, M. T. Int. Symp. on Toughness, Fracture and Fatigue of Polymers and Composites, Yamagata Univ., Japan, 1990, Abstract, p. 90
11 Yee, A. F., Pearson, R. A. and Sue, H. J. *Adv. Fract. Res.* 1989, **4**, 2739
12 Wu, S. *J. Polym. Sci., Polym. Phys. Edn.* 1983, **21**, 699
13 Hobbs, S. Y., Bopp, R. C. and Watkins, V. H. *Polym. Eng. Sci.* 1983, **3** (7), 380
14 Borggreve, R. J. M., Gaymans, R. J., Schijer, J. and Ingen-Housz, J. F. *Polymer* 1987, **28**, 1489
15 Ishikawa, M. *Kobunshi Ronbunshu* 1990, **47**, 83
16 Hobbs, S. Y. *Polym. Eng. Sci.* 1986, **26** (1), 74
17 Michler, G. H. *Integr. Fundam. Polym. Sci. Technol.* 1990, **5**, 61
18 Wu, S. *J. Appl. Polym. Sci.* 1988, **35**, 549
19 Michler, G. H. *Acta Polym.* 1993, **44**, 113
20 Kurauchi, T. and Ohta, T. *J. Mater. Sci.* 1984, **19**, 1699
21 Fujita, Y., Koo, K.-K., Angola, J. C., Inoue, T. and Sakai, T. *Kobunshi Ronbunshu* 1986, **43**, 119
22 Angola, J. C., Fujita, Y., Sakai, T. and Inoue, T. *J. Polym. Sci. (B)* 1988, **26**, 807
23 Koo, K.-K., Inoue, T. and Miyasaka, K. *Polym. Eng. Sci.* 1985, **25** (12), 741
24 Quingying, C., Wenjun, Z. and Fritz, H.-G. PPS Sixth Annual Meeting, Nice, France, 1990, Abstract, P07–11
25 Swisher, G. M. and Mathis, R. D. *Plast. Eng.* 1984, **6**, 53
26 Bi, L.-K. and Fetters, L. J. *Macromolecules* 1976, **9** (5), 732
27 Yamaoka, I. and Kimura, M. *Polymer* 1993, **34**, 4399
28 Löwenhaupt, B. and Hellmann, G. P. *Polymer* 1991, **32**, 1065
29 Koizumi, S., Hasegawa, H. and Hashimoto, T. *Makromol. Chem., Macromol. Symp.* 1992, **62**, 75
30 Massa, D. J. *Adv. Chem. Ser.* 1979, **176**, 433
31 Nishimoto, M., Keskkula, H. and Paul, D. R. *Polymer* 1989, **30**, 1279
32 Nishimoto, M., Keskkula, H. and Paul, D. R. *Polymer* 1991, **32**, 1274
33 Braun, D., Yu, D., Kohl, P. R., Gao, X., Andradi, L. N., Manger, E. and Hellmann, G. P. *J. Polym. Sci. (B)* 1992, **30**, 577
34 Kambour, R. P., Bendler, J. T. and Bopp, R. C. *Macromolecules* 1983, **16**, 753
35 ten Brinke, G., Karasz, F. E. and MacKnight, W. J. *Macromolecules* 1983, **16**, 1827
36 Kim, W. N. and Burns, C. M. *Macromolecules* 1987, **20**, 1876
37 Kim, W. N. and Burns, C. M. *Polym. Eng. Sci.* 1988, **28** (17), 1115
38 Fekete, E., Pukánszky, B. and Peredy, Z. *Angew. Makromol. Chem.* 1992, **199**, 87
39 Akiyama, S., Inoue, T. and Nishi, T. 'Polymer Blend: Compatibility and Interface', 1st Edn., CMC, Tokyo, 1981, p. 197
40 Inoue, T. and Meier, D. J. *Polym. Prepr. Japan* 1975, 346
41 Koizumi, S., Hasegawa, H. and Hashimoto, T. *Makromol. Chem., Macromol. Symp.* 1992, **62**, 75
42 Hashimoto, T., Tanaka, H. and Hasegawa, H. *Macromolecules* 1990, **23**, 4378
43 Kinning, D. J., Winey, K. I. and Thomas, E. L. *Macromolecules* 1988, **21**, 3502
44 Cheng, P.-L., Berney, C. V. and Cohen, R. E. *Makromol. Chem.* 1989, **190**, 589
45 Gebizlioglu, O. S., Argon, A. S. and Cohen, R. E. *Polymer* 1985, **26**, 529
46 Kijima, Y. and Kawaki, T. *Nikkei New Materials*, 26 Sept. 1988, 56
47 Ayano, R. and Murakawa, T. *Kobunshi Kagaku* 1972, **29** (330), 723
48 Erwin, L. SPE ANTEC, Washington, DC, 1978, p. 488
49 Erwin, L. *Polym. Eng. Sci.* 1978, **18** (7), 572
50 Tadmor, Z. *J. Appl. Polym. Sci.* 1974, **18**, 1753
51 Argon, A. S., Cohen, R. E., Jang, B. Z. and Vander Sande, J. B. *J. Polym. Sci., Polym. Phys. Edn.* 1981, **19** (2), 253